

<https://helda.helsinki.fi>

Atmospheric Fate of Monoethanolamine : Enhancing New Particle Formation of Sulfuric Acid as an Important Removal Process

Xie, Hong-Bin

2017-08-01

Xie , H-B , Elm , J , Halonen , R , Myllys , N , Kurten , T , Kulmala , M & Vehkamäki , H 2017 , ' Atmospheric Fate of Monoethanolamine : Enhancing New Particle Formation of Sulfuric Acid as an Important Removal Process ' , Environmental Science & Technology , vol. 51 , no. 15 , pp. 8422-8431 . <https://doi.org/10.1021/acs.est.7b02294>

<http://hdl.handle.net/10138/299835>

<https://doi.org/10.1021/acs.est.7b02294>

acceptedVersion

Downloaded from Helda, University of Helsinki institutional repository.

This is an electronic reprint of the original article.

This reprint may differ from the original in pagination and typographic detail.

Please cite the original version.

1 **The Atmospheric Fate of Monoethanolamine:**
2 **Enhancing New-particle Formation of Sulfuric Acid as**
3 **an Important Removal Process**

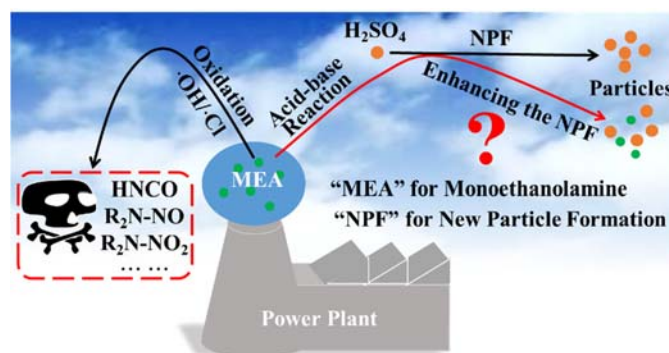
4 Hong-Bin Xie^{†‡}, Jonas Elm[‡], Roope Halonen[‡], Nanna Myllys[‡], Theo Kurtén[§], Markku
5 Kulmala[‡] and Hanna Vehkamäki[‡]

6 [†]Key Laboratory of Industrial Ecology and Environmental Engineering (Ministry of
7 Education), School of Environmental Science and Technology, Dalian University of
8 Technology, Dalian 116024, China

9 [‡]Department of Physics, University of Helsinki, P. O. Box 64, FIN-00014 Helsinki,
10 Finland

11 [§]Department of Chemistry, University of Helsinki, P. O. Box 55, FIN-00014 Helsinki,
12 Finland

13 Table of Contents (TOC)



14
15 **ABSTRACT.** Monoethanolamine (MEA), a potential atmospheric pollutant from
16 capture unit of a leading CO₂ capture technology, could be removed by participating
17 H₂SO₄-based new particle formation (NPF) as simple amines. Here we evaluated the
18 enhancing potential of MEA on H₂SO₄-based NPF by examining the formation of
19 molecular clusters of MEA and H₂SO₄ using a combined quantum chemistry

20 calculations and kinetics modeling. The results indicate that MEA at ppt-level can
21 enhance H₂SO₄-based NPF. The enhancing potential of MEA is < dimethylamine
22 (DMA), one of the strongest enhancing agents, and >> methylamine (MA), in contrast
23 to the order suggested solely by their basicity (MEA < MA < DMA). The unexpectedly
24 high enhancing potential is attributed to the role of -OH of MEA in increasing cluster
25 binding free energies by acting as both hydrogen bond donor and acceptor. After the
26 initial formation of one H₂SO₄ and one MEA cluster, the cluster growth mainly
27 proceeds by first adding one H₂SO₄, and then one MEA, which differs from growth
28 pathways in H₂SO₄-DMA and H₂SO₄-MA systems. Importantly, the effective removal
29 rate of MEA due to participation in NPF is comparable to that of oxidation by hydroxyl
30 radicals at 278.15 K, indicating NPF as an important sink for MEA.

31 INTRODUCTION

32 Monoethanolamine (MEA, NH₂CH₂CH₂OH) is a benchmark and widely utilized
33 solvent in amine-based postcombustion CO₂ capture (PCC) technology.¹⁻⁹ Given the
34 possible large-scale implementation of amine-based PCC, it is likely that there will be
35 relatively significant emissions of MEA or other alkanolamines to the atmosphere from
36 PCC units due to their relatively high vapor pressure.¹⁰ It has been estimated that a CO₂
37 capture plant which removes 1 million tons CO₂ per year from flue gas using MEA as
38 solvent could potentially emit 80 tons MEA into the atmosphere.^{11,12} Therefore, in
39 recent years concern about the atmospheric fate of the representative amine MEA has
40 been increasing,^{6,13-22} as MEA could potentially form an environmental risk.^{11,12,17}

41 Several studies have addressed the removal of MEA by atmospheric oxidation.^{6,13-}
42 ²² The oxidation by hydroxyl radicals ($\cdot\text{OH}$) has been considered to be its main
43 degradation pathway, followed by chlorine radicals ($\cdot\text{Cl}$) at daytime.¹³ The nitrate
44 radical may play a significant role in MEA oxidation at night, though very little is
45 known about this pathway. The reaction rate constants of MEA with $\cdot\text{OH}$ and $\cdot\text{Cl}$ are
46 in the order of 10^{-11} and 10^{-10} $\text{cm}^3 \text{ molecule}^{-1} \text{ s}^{-1}$, respectively, translating to 2.6-3.6
47 hours atmospheric lifetime.^{6,13,14,18,19} More importantly, atmospheric oxidation of MEA
48 by $\cdot\text{OH}$ and $\cdot\text{Cl}$ can produce potentially hazardous compounds (such as isocyanic acid,
49 HNCO, nitramine and nitrosamine),^{6,13,19} which can increase the environmental risk of
50 MEA emission. Besides oxidation, acid-base reaction could be another important sink
51 for MEA. However, the atmospheric fate related to the basicity of MEA has received
52 little attention until now.

53 Atmospheric aerosol particles, at least 50% of which originates from new-particle
54 formation (NPF), are known to affect human health and remain one of the leading
55 uncertainties in global climate modeling and prediction.²³⁻²⁷ Many studies have shown
56 that atmospheric bases such as ammonia and amines stabilize sulfuric acid clusters in
57 the lower troposphere via acid-base reactions, and therefore enhance H_2SO_4 -based NPF
58 rates.^{25,28-42} Compared to ammonia, amines, including monomethylamine (MA),
59 dimethylamine (DMA) and trimethylamine (TMA), can bind much more strongly to
60 sulfuric acid molecules^{29,40-43} and thus can efficiently enhance clustering sulfuric
61 acid.⁴³ Recent work by Almeida et al. performed at the CLOUD chamber at CERN

62 shows that 5 ppt of dimethylamine can enhance NPF rates more than 10000 times
63 compared with the case of 5 ppt ammonia, and is sufficient to produce particle
64 formation rates of the same order of magnitude as observed in the atmosphere.²⁵
65 Besides ammonia, MA, DMA and TMA, atmospheric diamines were recently found to
66 efficiently enhance NPF.^{44,45}

67 In a similar fashion to simple alkylamines, MEA can potentially influence NPF
68 via acid-base reactions and therefore participating in NPF could be another atmospheric
69 sink of MEA. A recent study highlighted the possible role of emitted amines from CO₂
70 capture unit of PCC in enhancing NPF.²⁵ The basicity of MEA is higher than that of
71 ammonia and lower than that of methylamine and dimethylamine (pK_b values of MEA
72 4.50, MA 3.36, DMA 3.29, ammonia 5.7).⁴⁶ If judged solely by the basicity, MEA
73 should have a higher enhancing effect on H₂SO₄-based NPF than NH₃, and lower effect
74 than MA and DMA when atmospheric concentration of MEA is assumed to be similar
75 to that of NH₃, MA and DMA. From the point of molecular structure, MEA has
76 additional -OH compared to ammonia, MA and DMA. When forming clusters between
77 MEA and H₂SO₄, the -OH group in MEA can form additional hydrogen bonds (H-
78 bonds), which increase the binding energy of MEA with H₂SO₄. The conflicting effects
79 of one favorable (more H-bonds) and one unfavorable factor (decreased basicity
80 compared with methylamine and dimethylamine) could make it difficult to estimate
81 how strong the enhancing effect of MEA will be. No previous studies have considered
82 the potential role of alkanolamines in NPF involving H₂SO₄. An additional -OH in the

83 amine may lead to a different NPF pathway and rate compared to the
84 ammonia/MA/DMA-H₂SO₄ systems. Therefore, to obtain a complete view of the
85 atmospheric fate of MEA and extend the current knowledge of NPF involving amines
86 and H₂SO₄, information about the potential of MEA to participate in atmospheric NPF
87 is crucial.

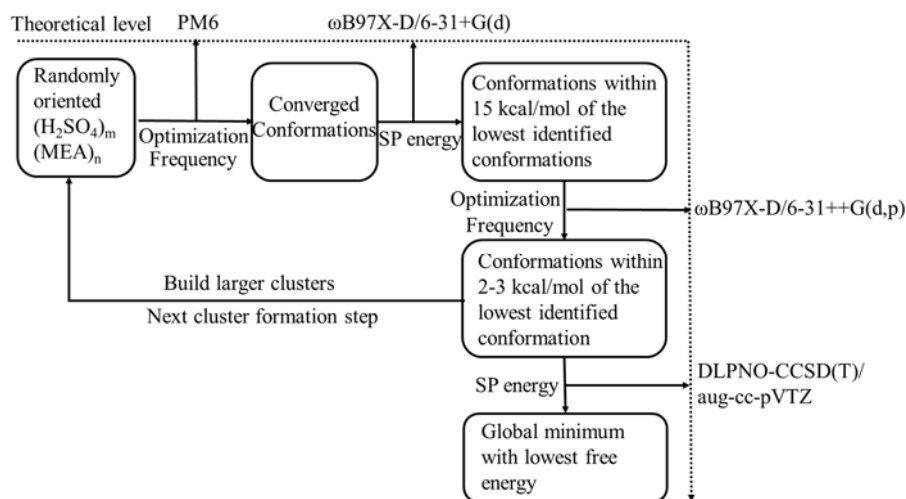
88 In this study, we investigate the initial step of atmospheric H₂SO₄-based NPF by
89 examining the formation of molecular clusters of MEA and sulfuric acid using a
90 combination of quantum chemistry calculations and kinetics modeling employing the
91 Atmospheric Cluster Dynamics Code^{47,48} (ACDC). Via systematic conformational
92 searches, we have obtained minimum free energy structures of clusters of composition
93 (MEA)_m(SA)_n ($m=0-4$ and $n=1-4$, “SA” represents H₂SO₄). The corresponding
94 thermodynamic data and previously reported results for pure sulfuric acid (SA)₁₋₄
95 clusters⁴⁹ are used in ACDC to obtain cluster formation pathways and kinetics in the
96 MEA-H₂SO₄ system. In addition, the effect of hydration on the cluster formation
97 kinetics of MEA and H₂SO₄ is considered.

98 **COMPUTATIONAL DETAILS**

99 **Electronic Structure Calculations.** The most critical parameters in identifying cluster
100 formation pathways and kinetics are the cluster formation free energies. Both minimum
101 free energy structures of clusters (MEA)_m(SA)_n ($m=0-4$ and $n=0-4$) and computational
102 method will determine the reliability of calculated cluster formation free energies. Here,
103 a global minimum sampling technique (Figure 1), which has previously been applied

104 to study atmospheric cluster formation,^{45,50,51} was used to search for the global minima
105 of clusters (MEA)_m(SA)_n(*m*=1-4 and *n*=0-4). The pure (SA)₁₋₄ clusters were taken from
106 the work of Ortega et al.⁴⁹ In Figure 1, all optimizations, frequency or single point
107 energy calculations with density functional theory and semiempirical PM6 level have
108 been performed in GAUSSIAN 09.⁵² The ωB97X-D functional was selected as the core
109 optimization and frequency calculation method in Figure 1, since it has shown good
110 performance for studying the formation of atmospheric molecular clusters.^{53,54} Single
111 point energy calculations at DLPNO-CCSD(T) (Domain-based local pair natural orbital
112 coupled cluster^{55,56})/aug-cc-pVTZ level have been performed in ORCA version 3.0.3.⁵⁷
113 Recent studies indicated that the DLPNO-CCSD(T) method can be used to calculate
114 atmospheric acid-base clusters up to 10 molecules⁵⁸ and the utilized DLPNO-
115 CCSD(T)/aug-cc-pVTZ method has been shown to yield a mean absolute error of 0.3
116 kcal/mol compared to CCSD(T) complete basis set estimates, based on a test set of 11
117 small atmospheric cluster reactions⁵⁴. The MEA monomer has 13 conformations^{6,59} and
118 each was used as a starting point for forming the molecular clusters. For the global
119 minimum search, more than 10000 randomly oriented configurations were built for
120 each cluster. We have estimated the Gibbs free energies for all obtained global minima
121 at 298.15 K by combining the single point energies at the DLPNO-CCSD(T)/aug-cc-
122 pVTZ level and Gibbs free energy correction terms at the ωB97X-D/6-31++G(d,p)
123 level. The formation free energies for each cluster were obtained by subtracting Gibbs
124 free energy of the constituent molecules from that of the cluster at 298.15 K. The

125 formation free energies at other temperatures were calculated under the assumption that
 126 enthalpy and entropy change remain constant in the tropospheric temperature range.



127
 128 Figure 1. Flowchart for the multistep global minimum sampling method. “SP”
 129 represents a single point energy calculation.

130 To consider the effect of hydration, the $(\text{MEA})_m(\text{SA})_n\text{W}_x$ ($m=0-2$, $n=0-2$, $x=1-3$,
 131 “W” represents H_2O) clusters were investigated. For their global minimum search, a
 132 similar scheme as for the clusters without water molecules was used. In addition, to
 133 directly compare the enhancing effect of MEA to ammonia, MA and DMA, we re-
 134 evaluated their formation free energies at the same theoretical level, based on reported
 135 cluster structures, or new lower energy structures (presented in Figure S1).^{48, 49, 60} It
 136 should be noted that for global minimum of the unhydrated MA-SA clusters, only
 137 $(\text{MA})_{0-3}(\text{SA})_{0-3}$ is available^{41,60} and therefore formation free energy data for MA are
 138 only for $(\text{MA})_{0-3}(\text{SA})_{0-3}$.

139 **ACDC model.** We used ACDC to study the formation pathways, steady-state
 140 concentrations and formation rates of clusters. The detailed theory behind the ACDC

141 was present in a study by McGrath et. al.⁴⁷ Briefly, the code generates equations for the
142 time derivatives of the concentrations of all studied clusters, and uses the Matlab ode15s
143 routine to solve differential equations and simulate the time-dependent cluster
144 concentrations. The differential equations, also called birth-death equations, include
145 source terms from collisions of smaller clusters and evaporations from larger clusters,
146 and sink terms from collisions with other clusters and evaporations into smaller clusters.
147 In addition, the cluster formation rate in ACDC is defined as the flux of clusters outside
148 the system. Whether a cluster is allowed to be outside the system or not is judged by
149 the boundary condition. The hydration effect was considered in ACDC by taking H₂O
150 molecule as an environment to affect the collision or evaporation of base-acid cluster.⁶¹
151 The simulated system is a “4 × 4 box” for unhydrated system, where 4 is the maximum
152 number of H₂SO₄ or MEA molecules in the clusters. The (MEA)₄(SA)₅ and
153 (MEA)₅(SA)₅ were allowed to grow out of the system and all other clusters crossing the
154 box edge are brought back to the simulation box by monomer evaporations (see
155 boundary condition in Supporting Information (SI)). The ACDC simulations were
156 primarily run at 278.15 K, with additional runs performed at 258.15, 268.15, 288.15
157 and 298.15 to study the temperature effect. A constant coagulation sink coefficient of
158 $2.6 \times 10^{-3} \text{ s}^{-1}$ was used as sink term. This value corresponds to typical one observed in
159 boreal forest environments.⁴⁸ The sulfuric acid concentration was set to be 10^5 , 10^6 , 10^7 ,
160 10^8 and 10^9 cm^{-3} , a range relevant to atmospheric NPF.^{25,48,62} Atmospheric MEA
161 concentrations were set to be 1, 10, and 100 ppt, a range relevant to atmospheric NPF

162 for DMA.²⁵ It should be mentioned that the acid concentration $[\text{H}_2\text{SO}_4]$ was defined as
163 the total concentration of all neutral clusters containing one acid and any number of
164 base molecules, as in a previous study.⁴⁸ When hydration effect was considered, the
165 simulated system is “ 2×2 box”. Average collision and evaporation coefficients over
166 the hydrate distribution for each cluster of $(\text{MEA})_m(\text{SA})_n$ ($m=0-2$, $n=0-2$) were used in
167 the birth-death equations for $[\text{H}_2\text{SO}_4] = 10^6$ and $[\text{MEA}] = 10$ ppt and at 278.15 K. The
168 equilibrium hydrate distribution for each cluster was calculated by the equilibrium
169 constant for the formation of the respective hydrate.⁶¹ Similar to the definition of
170 boundary condition of unhydrated MEA-SA cluster, the $(\text{MEA})_2(\text{SA})_3$ and
171 $(\text{MEA})_3(\text{SA})_3$ were allowed to grow out of the system. As a comparison, we also
172 performed ACDC simulation for MA- H_2SO_4 and DMA- H_2SO_4 systems at 278.15 K.
173 The simulated system is a “ 3×3 box” for MA since only $(\text{MA})_{0-3}(\text{SA})_{0-3}$ is available,
174 and “ 4×4 box,” for DMA. The $(\text{MA})_3(\text{SA})_4$ and $(\text{MA})_4(\text{SA})_4$, and $(\text{DMA})_4(\text{SA})_5$ and
175 $(\text{DMA})_5(\text{SA})_5$ were allowed to grow out of the simulation box for MA- H_2SO_4 and
176 DMA- H_2SO_4 system (see SI), respectively. Other ACDC simulation details are similar
177 to those for MEA. In addition, ACDC simulation was performed for MEA- H_2SO_4 with
178 3×3 box, to compare with MA- H_2SO_4 system with a similar simulation box size.

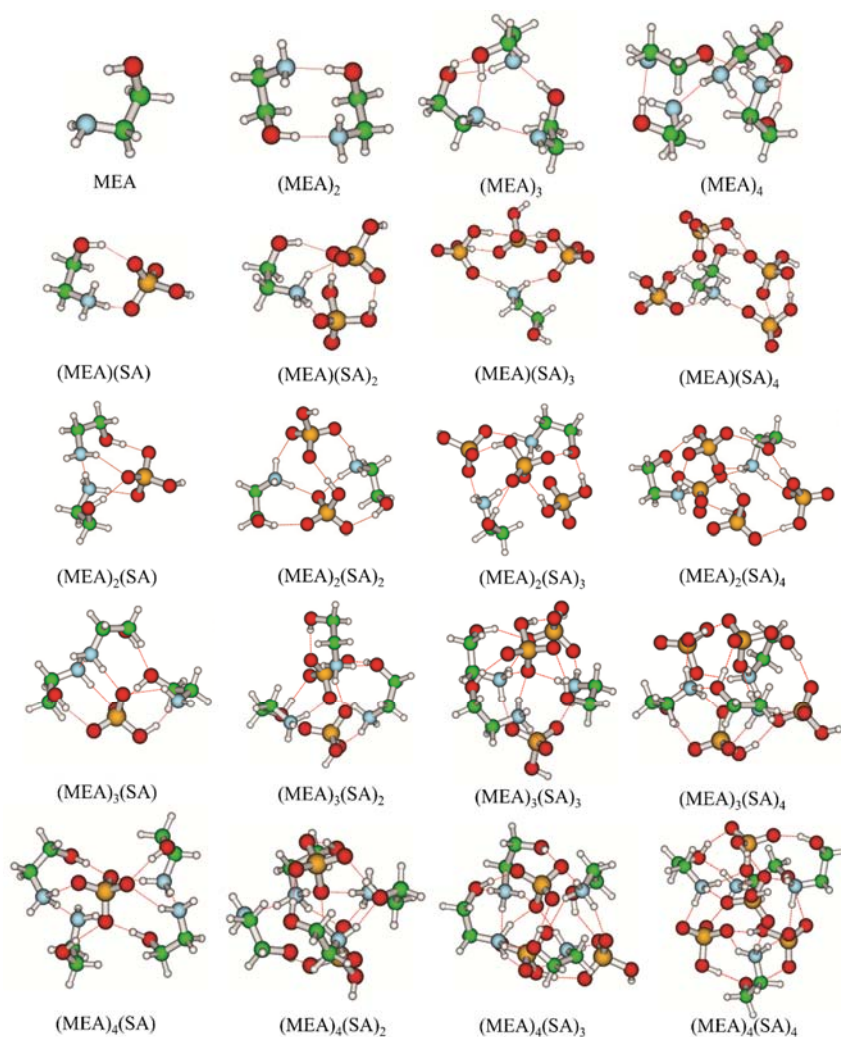
179 **RESULTS AND DISCUSSION**

180 **Structures and Thermodynamic Data.** We use $(\text{MEA})_m(\text{SA})_n$ to represent the cluster
181 formed by m MEA molecules and n H_2SO_4 molecules to avoid explicitly specifying the
182 proton transfer status. Since previous studies have discussed the structures of pure

183 H₂SO₄ clusters,⁴⁹ here, we mainly focus on the clusters (MEA)_m(SA)_n($m=1-4$ and $n=0-$
184 4). The structures of (MEA)_m(SA)_n($m=1-4$ and $n=0-4$) are shown in Figure 2. Generally,
185 in the homo-molecular clusters (MEA)_m($m=1-4$), no proton transfer has occurred and
186 clusters are stabilized mainly by H-bonds. In all hetero-molecular clusters, proton
187 transfer is observed, and clusters are stabilized by both H-bonds and electrostatic
188 interaction between positive and negative species. When $n \geq m$, the amine (-NH₂)
189 groups of all MEA molecules are protonated by H₂SO₄. In this case H₂SO₄ only
190 transfers a single proton and in no cases a sulphate ion is formed. When $n < m$, there
191 are two different proton transfer pattern. For (MEA)₂(SA), (MEA)₃(SA) clusters, none
192 or one of the protons of H₂SO₄ are donated, and therefore not all MEA molecules are
193 protonated. For (MEA)₄(SA), (MEA)₄(SA)₂, (MEA)₄(SA)₃ and (MEA)₃(SA)₂, H₂SO₄
194 can donate two protons, and therefore all MEAs are protonated in the case of $m - n = 1$
195 ((MEA)₄(SA)₃ and (MEA)₃(SA)₂), while MEA is not completely protonated in the case
196 of $m - n > 1$ ((MEA)₄(SA) and (MEA)₄(SA)₂). The above proton transfer patterns for
197 H₂SO₄-MEA clusters are similar to those of H₂SO₄-DMA clusters.^{48,49}

198 Another structural feature in all clusters except (MEA)(SA)₃ is that -OH
199 groups of all MEAs can form at least one H-bond with H₂SO₄ as H-bond donors. In
200 many cases such as (MEA)₃, (MEA)₄, (MEA)(SA)₄, (MEA)₂(SA)₃, (MEA)₂(SA)₄,
201 (MEA)₃(SA)₁, (MEA)₃(SA)₂, (MEA)₃(SA)₄, (MEA)₃(SA)₂, (MEA)₄(SA)₂ and
202 (MEA)₄(SA)₃ clusters, the -OH group of MEA can form another H-bond with the -OH
203 group of H₂SO₄, ammonium cation (-RNH₃⁺) of protonated MEA or -OH of MEA as a

204 H-bond acceptor. The involvement of the -OH group of MEA leads to a preference for
 205 a spherical three-dimensional structure, especially for the large studied cluster sizes. As
 206 an exception (MEA)(SA)₃, we also located a low-energy minimum (Figure S2)
 207 involving H-bonds where -OH group of MEA acts as both a hydrogen bond donor and
 208 acceptor. However, the configuration is not the global minimum for the Gibbs free
 209 energy. The binding energy of this minimum is about 1 kcal/mol lower than that of the
 210 free energy global minimum shown in Figure 2, and thus unfavorable entropy effects
 211 are taking place in this configuration.



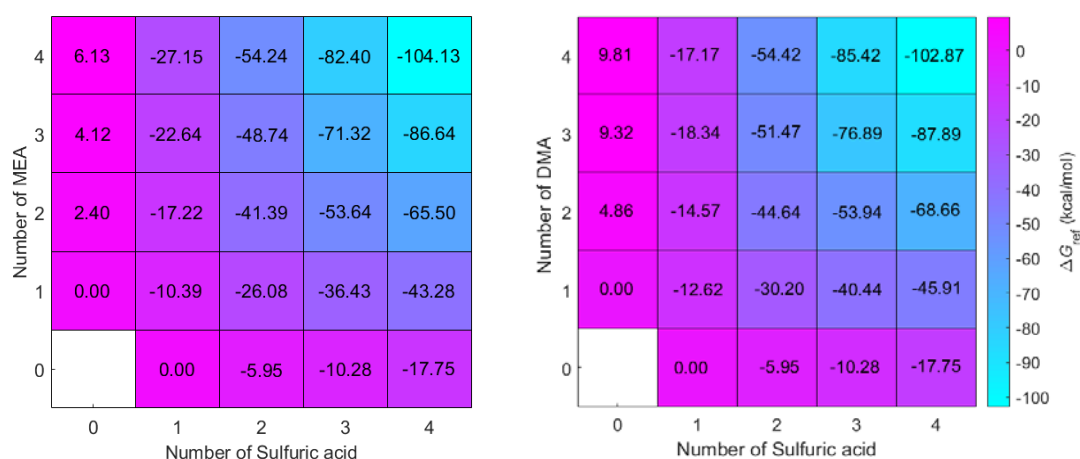
212

213 Figure 2. The Structures of global free energy minima for (MEA)_m(H₂SO₄)_n ($m=1-4$ and

214 $n=0-4$) at the ω B97X-D/6-31++G(d,p) level of theory. The red ball represents oxygen
215 atom, blue is nitrogen atom, green is carbon atom and white is hydrogen atom.

216 It is known that DMA is one of the strongest agents for enhancing atmospheric
217 H₂SO₄-based NPF.^{25,29,43} Here, we take formation free energies of the H₂SO₄-DMA
218 system as a reference to discuss the formation free energies of H₂SO₄-MEA. The free
219 energy data at 298.15 K for the formation of the clusters from their constituent
220 molecules for the MEA/DMA-H₂SO₄ system are presented in Figure 3, and the
221 corresponding thermodynamical quantities ΔH and ΔS are presented in Table S1. For
222 the pure base clusters, formation free energy of all MEA clusters is lower than that of
223 corresponding DMA clusters. This results from the fact that there is one more H-bond
224 bonding agent (-OH) in MEA compared with DMA, which leads to more H-bonds in
225 the pure MEA clusters than that in the corresponding DMA clusters. The formation free
226 energy for most hetero-molecular H₂SO₄-MEA clusters is 0.2-5.6 kcal/mol higher than
227 that of corresponding H₂SO₄-DMA clusters. However, the formation free energy for
228 (MEA)₂SA, (MEA)₃SA and (MEA)₄SA and (MEA)₄(SA)₄ is lower than that of the
229 corresponding clusters from DMA. The difference in formation free energies of MEA
230 clusters, compared with DMA clusters, originates from the competition between the
231 unfavorable (lower basicity of MEA than that of DMA) and favorable factor (the
232 formation of more H-bonds from the -OH group of MEA) for forming clusters. In
233 addition, we noted that formation free energies of MEA-H₂SO₄ clusters are lower than
234 those of the corresponding MA-H₂SO₄ clusters (Figure S3) although basicity of MEA

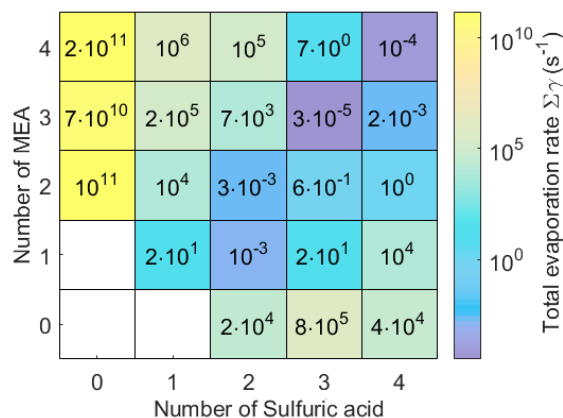
235 is much lower than that of MA, indicating that the -OH group in MEA does indeed play
 236 an important role in the cluster formation between MEA and H₂SO₄. In recent study,
 237 Chen et al. revealed that besides the basicity, the hydrogen-bonding capacity of -NH_x
 238 ($x = 1-3$) group in amine/ammonia can play an important role in enhancing
 239 methanesulfonic acid driven NPF.⁶³ Our findings and Chen et al.'s study⁶³ together
 240 show the importance of molecular interactions involving -NH_x ($x = 1-3$) group and other
 241 functional groups of amines in NPF. In addition, similar to MA and DMA, the
 242 formation free energies for MEA are much lower than those of NH₃ (Figure S3) with
 243 H₂SO₄.



244 Figure 3. Calculated formation free energies for (MEA)_m(SA)_n (left panel) and
 245 (DMA)_m(SA)_n (right panel) clusters ($m=0-4$ and $n=0-4$) at the DLPNO-CCSD(T)/aug-
 246 cc-pVTZ// ω B97X-D/6-31++G(d,p) level and 298.15 K and 1 atm (reference pressure
 247 of acid and base).

248 **Evaporation Rates.** In view of the acid-base cluster growth, the stability of the cluster
 249 can be deduced by comparing the evaporation rate with the collision rate, which mainly
 250 depends on the collision rate constant and the concentration of the acid and base

251 molecules. However, the collision rate constants for the studied clusters are very close
252 to each other and thus difference in the evaporation rate can be used to represent the
253 stability of clusters at the given acid and base concentration. The evaporation rates for
254 $(\text{MEA})_m(\text{SA})_n$ ($m=0-4$ and $n=0-4$) on the MEA-SA grid at 278.15 are presented in Figure
255 4. Generally, evaporation rates for clusters $(\text{MEA})_2(\text{SA})_2$, $(\text{MEA})_1(\text{SA})_2$, $(\text{MEA})_3(\text{SA})_3$,
256 $(\text{MEA})_3(\text{SA})_4$ and $(\text{MEA})_4(\text{SA})_4$ are of the order of 10^{-3} - 10^{-5} s^{-1} , which is much lower
257 than those for other studied cluster sizes. When the concentration of MEA or H_2SO_4 is
258 around or above ppt level, those clusters with evaporation rate 10^{-3} - 10^{-5} s^{-1} can be
259 considered to be stable and $(\text{MEA})_3(\text{SA})_3$ and $(\text{MEA})_4(\text{SA})_4$ are the most stable clusters
260 (see discussion on stability of clusters in SI). By checking all evaporation pathways
261 (see Table S2), evaporation of a H_2SO_4 or MEA monomer is found to be the main decay
262 route for all clusters studied here. If m and n are unequal, evaporation of species with
263 greater number of molecules is always preferred. For clusters with $m = n > 2$,
264 evaporation of MEA is faster than that of H_2SO_4 . In addition, when there is equal
265 number of molecules in two clusters, the evaporation rate of MEA abundant cluster is
266 higher than corresponding H_2SO_4 abundant cluster, indicating that the bonding ability
267 of H_2SO_4 to the cluster is stronger than that of MEA. A similar phenomena concerning
268 the stronger bonding ability of acid is also found in other acid-base cluster systems,
269 such as DMA-SA, NH_3 - H_2SO_4 , and NH_3 - HNO_3 .^{49,64}



270

271 Figure 4. The evaporation rates for $(\text{MEA})_m(\text{SA})_n$ ($m=0-4$ and $n=0-4$) on the MEA-SA
 272 grid at 278.15.

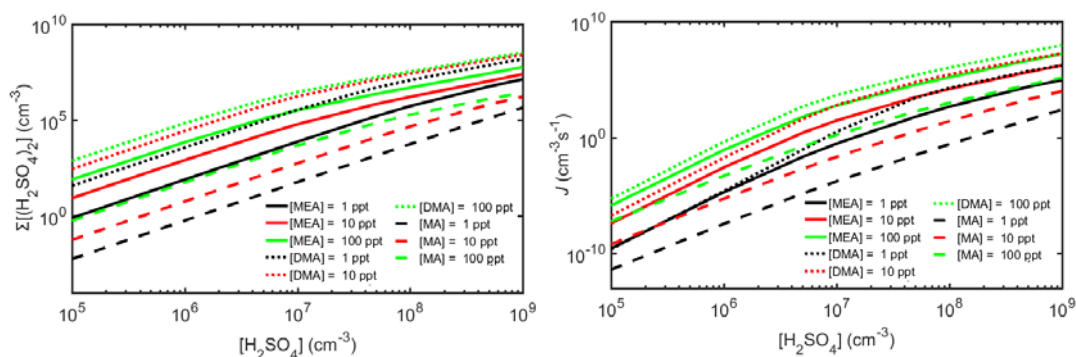
273

It is also interesting to compare cluster evaporate rates for the different amines
 274 (MA, DMA and MEA) at the same simulation condition. For most of the clusters,
 275 including hetero-molecular and pure base clusters, the evaporation rates for MEA
 276 clusters are lower than corresponding ones for MA (Figure S4) and DMA (Figure S4)
 277 clusters. However, it is not straightforward to conclude which amine can form the most
 278 stable clusters as evaporation rates for a couple of clusters with MA and DMA are lower
 279 than those of MEA clusters. If the initially formed one SA and one base cluster (which
 280 are crucial for cluster growth at relevant H_2SO_4 and base concentration for MEA, MA
 281 and DMA as discussed in the Growth Pathways section) are compared, evaporate rate
 282 of $(\text{MEA})(\text{SA})$ is lower than that of $(\text{MA})(\text{SA})$ and higher than that of $(\text{DMA})(\text{SA})$.
 283 Therefore, the stability of initially formed clusters for the three types of amine- H_2SO_4
 284 clusters follows the trend $(\text{DMA})(\text{SA}) > (\text{MEA})(\text{SA}) > (\text{MA})(\text{SA})$ at the given acid and
 285 base concentrations. In addition, in accordance with a previous study,⁴⁷ the evaporation
 286 of small clusters is found to be the main decay route for some of DMA- H_2SO_4 clusters.

287 This is not the case for MEA-SA and MA-SA clusters, where monomer evaporation is
288 dominant. This results from the higher stability of the small DMA-H₂SO₄ clusters.

289 **Steady-state Cluster Concentrations and Formation Rates.** The steady-state sulfuric
290 acid dimer concentration (all clusters including sulfuric acid dimer) and the formation
291 rate of clusters growing out of the simulation box can be taken as two important
292 quantities characterizing the stabilization potential of a given base in H₂SO₄-based
293 NPF.^{25,43,60} Figure 5 shows the steady-state sulfuric acid dimer concentration and the
294 cluster formation rate as a function of monomer concentration (H₂SO₄ concentration in
295 the range 10⁵ - 10⁹ cm⁻³, MEA mixing ratios of 1-100 ppt) at 278.15 K for MEA-H₂SO₄
296 clusters, along with DMA-H₂SO₄ and MA-H₂SO₄ clusters as a comparison. Generally,
297 the sulfuric acid dimer concentration and the cluster formation rate increase with
298 increasing the concentrations of MEA and H₂SO₄ at the considered condition. The
299 MEA concentration dependence of the sulfuric acid dimer concentration and the cluster
300 formation rate weakens with increasing H₂SO₄ concentration, indicating that the system
301 gradually approaches saturation with respect to MEA at a high H₂SO₄ concentration.
302 Similar behavior is also found in the simulations with MA and DMA as base. More
303 importantly, MEA yields roughly 10–10²-fold dimer concentration and 10²–10³-fold
304 formation rate compared to the simulations with MA as a base, and 0.02-0.2-fold dimer
305 concentration and 0.02–1-fold formation rate as compared to the simulations with DMA
306 as a base, indicating the order of the stabilization potential of these three amines
307 follows: DMA > MEA > MA. It deserves mentioning that MEA-H₂SO₄ formation rates

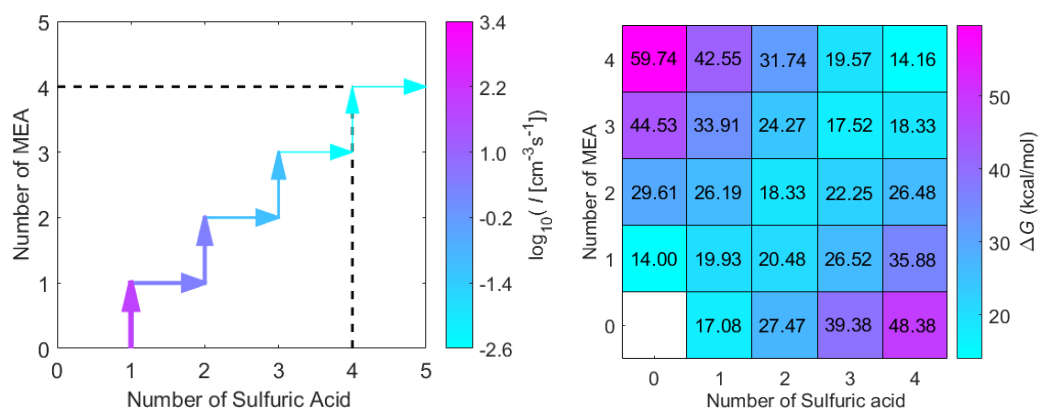
308 compared to MA-H₂SO₄ become even higher if the same simulation box size is used
 309 for MEA and MA (3 × 3) (formation rate of MEA-H₂SO₄ will increase 1.1-6 times,
 310 compared with 4 × 4 box). However, the difference in sulfuric acid dimer concentration
 311 was similar with different simulation box sizes. As experimental evidence has shown
 312 that DMA and MA have an enhancing effect on H₂SO₄-based NPF at ppt level,^{25,43} it
 313 can be expected that MEA will have a similar effect with magnitude in between DMA
 314 and MA. Therefore, we can conclude that MEA can enhance NPF of H₂SO₄ when the
 315 atmospheric concentration of MEA reaches ppt level. The higher stabilization potential
 316 of MEA, compared with MA, further verifies the important role of the -OH group of
 317 MEA in enhancing NPF involving H₂SO₄, as the basicity of MEA is lower than that of
 318 MA. In addition, both the sulfuric acid dimer concentration and the formation rate
 319 present negative temperature dependence in the range of 260-300 K, relevant to
 320 tropospheric conditions as shown in Figure S5. The negative temperature dependence
 321 effect is more prominent at lower MEA (1 ppt) and lower H₂SO₄ concentrations (10⁶
 322 cm⁻³).



323
 324 Figure 5. Simulated steady-state H₂SO₄ dimer concentration $\Sigma[(\text{H}_2\text{SO}_4)_2]$ (cm⁻³) (left
 325 panel) and the cluster formation rate J (cm⁻³s⁻¹) out of the simulation system (right

326 panel) as a function of monomer concentration at 278.15 K.

327 **Growth Pathways.** Figure 6 presents the growth pathway and the actual Gibbs free
328 energy surface⁴⁷ for MEA and H₂SO₄ clusters at [H₂SO₄] = 10⁶ cm⁻³, [MEA] = 10 ppt
329 and 278.15 K. The actual Gibbs free energy surface was obtained by converting the
330 change of free energy from 1 atm to the actual vapor pressures of the components.⁴⁷ As
331 can be seen in Figure 6 (left panel), the first step in the growth is the binding of one
332 H₂SO₄ molecule to a MEA molecule. After the initial step, the growth mainly proceeds
333 by firstly adding one H₂SO₄, and then one MEA. The main flux out of the system is the
334 (MEA)₄(SA)₅ cluster. Combining the growth pathway with the actual Gibbs free energy
335 surface (right panel in Figure 6), two features can be observed. First, clusters do not
336 follow the lowest free energy pathways ((MEA)₁(SA)₁→(MEA)₂(SA)₂→(MEA)₃(SA)₃
337 →(MEA)₄(SA)₄), which would involve the cluster collision with (MEA)₁(SA)₁ cluster.
338 This results from fact that the concentration of the (MEA)₁(SA)₁ cluster (5.73×10^3 cm⁻³)
339 ³) is much lower than that of the H₂SO₄ monomer (9.94×10^5 cm⁻³). Secondly, the
340 addition of H₂SO₄ monomers involves a small free energy barrier, but the addition of
341 MEA does not. Furthermore, combining the growth pathway with the evaporation rate
342 of the clusters, we can conclude that the formation of initial cluster (MEA)₁(SA)₁ is the
343 rate-determining step for the cluster growth since the (MEA)₁(SA)₁ cluster is much
344 more unstable than other clusters in the cluster growth pathway and readily evaporates
345 back into MEA and SA monomers.



346 Figure 6. Main clustering pathways (left panel) and actual Gibbs free energy surface
 347 for the formation of clusters $\text{MEA}_m(\text{H}_2\text{SO}_4)_n$ ($m=0-4$ and $n=0-4$) (right panel) at 278.15
 348 K, $[\text{H}_2\text{SO}_4] = 10^6 \text{ cm}^{-3}$ and $[\text{MEA}] = 10 \text{ ppt}$. For figure clarity, the pathways
 349 contributing less than 5% to the flux of the cluster are not shown.

350 We also compared the growth pathways for $\text{MEA-H}_2\text{SO}_4$ with $\text{MA-H}_2\text{SO}_4$ and
 351 $\text{DMA-H}_2\text{SO}_4$ system at the same simulation condition. The formation pathways for
 352 $\text{MA-H}_2\text{SO}_4$ and $\text{DMA-H}_2\text{SO}_4$ are presented in Figure S6. A common feature is that the
 353 initially formed cluster mainly consists of one H_2SO_4 and one base molecule for all
 354 three amines. However, as a whole, the growth pathway for the $\text{MEA-H}_2\text{SO}_4$ system is
 355 significantly different from that of the $\text{MA-H}_2\text{SO}_4$ and $\text{DMA-H}_2\text{SO}_4$ systems. In
 356 accordance with a previous study,⁴⁷ collisions involving the $(\text{DMA})_1(\text{SA})_1$ cluster
 357 contribute significantly to the growth for DMA-SA system, which makes the growth
 358 occur mainly along the diagonal on the acid-base grid. In contrast to MEA and DMA ,
 359 the cluster growth for the MA system does not follow the diagonal direction and the
 360 formation of larger clusters $(\text{MA})_1(\text{SA})_2$ and $(\text{MA})_2(\text{SA})_3$ has two pathways either via

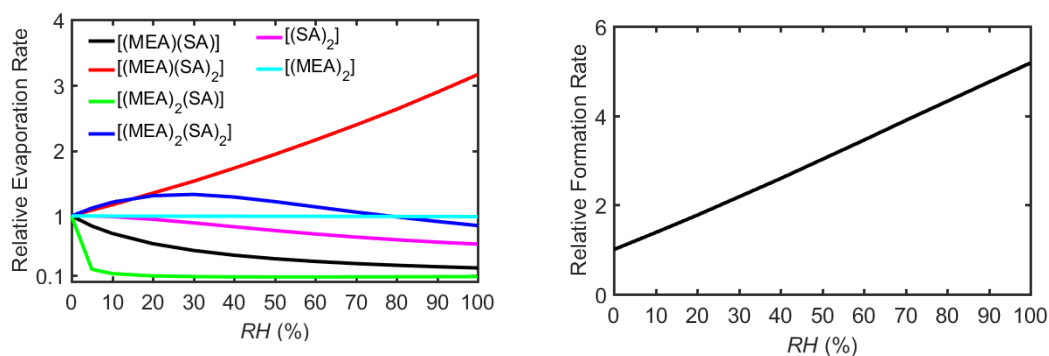
361 addition of H₂SO₄ or MA. The sulfuric acid dimer has a significant population in the
362 initial clusters, which results from the low stability of the (MA)₁(SA)₂ cluster.

363 **Effect of Hydration.** As water is many orders of magnitude more abundant than
364 sulfuric acid and bases in the atmosphere, hydration might change the cluster formation
365 free energies and therefore cluster formation kinetics^{61,65,66} Previous studies have found
366 that clusters consisting of H₂SO₄ and DMA or ammonia are mainly hydrated by less
367 than three H₂O molecules.^{30,61} We expected that MEA-H₂SO₄ clusters could still be
368 hydrated by less than three H₂O molecules although the structure of MEA is different
369 from DMA and ammonia. Here, 1-3 H₂O molecules were considered to study the effect
370 of hydration on the formation kinetics of MEA-H₂SO₄ clusters. In addition, to save
371 computational resources, we only selected the smallest clusters (MEA)_m(SA)_n ($m = 0-$
372 $2, n = 0-2$) as test system to investigate the hydration. Based on the calculated
373 equilibrium hydrate distribution of the clusters at relative humidities (RH) 20%, 50%
374 and 100%, at 278.15 K, converted from calculated Gibbs free energies of stepwise
375 hydration at 278.15 K and 1 atm, we can conclude that sulfuric acid-MEA clusters are
376 only mildly hydrated (0-2 H₂O molecules depending on RH). Details for the discussion
377 on calculated Gibbs free energies of stepwise hydration, optimized structures and the
378 hydrate distribution of the clusters are presented in SI. Here, we mainly focus on the
379 effect of hydration on the cluster formation kinetics.

380 In principle, hydration can affect the cluster formation rate both through the
381 collision and evaporation rates. However, hydration was found to have little effect on

382 the collision rate since the collision diameter, an important factor in collision rate
383 coefficients in kinetic collision theory employed in ACDC, changes very little with
384 hydration.⁶¹ Hence, only the effect of hydration on the evaporation rates and formation
385 rates will be discussed in detail. Figure 7 presents the evaporation rates (left) and
386 formation rates (right) as a function of RH at 278.15 K compared to dry conditions.
387 Clearly, the presence of water has various effects on the evaporation rate depending on
388 the given cluster. Water has a little effect on the evaporation rate of the (SA)₂ and
389 (MEA)₂(SA)₂ and almost no effect on that of the (MEA)₂ cluster. However, the
390 evaporation rate of (MEA)(SA)₂ can be increased up to 3 times by hydration, and that
391 of (MEA)₂(SA) can be decreased by 13 times compared to the dry case. More
392 importantly, the presence of water decreases the evaporation rate of initially formed
393 (MEA)(SA) clusters, i.e. the rate-determining step for cluster growth in the system, and
394 this trend gradually increases with RH, which explains the increased cluster formation
395 rate with increasing RH (right panel in Figure 7). The formation rate can be increased
396 about 5 fold at RH = 100 % compared to the dry case. It should be mentioned that
397 although the absolute formation rate obtained from a small simulation box (2 × 2) is not
398 reliable, the relative formation rate presented here should cancel out any significant bias
399 introduced by the small simulation box. Generally, from these small cluster hydration
400 simulations, we can conclude that hydration can slightly influence the evaporation rate,
401 but the effect is in all cases relatively low and does not severely influence the results.
402 Although it is not expected that qualitative conclusion from current study could be

403 changed when larger clusters and more water molecules are used, future study with
404 larger clusters and more water molecules is still deserved, to reach a more definitive
405 conclusion about the RH effect on MEA-H₂SO₄ cluster formation kinetics.



406 Figure 7. Relative evaporation rate (left panel) and cluster formation rate ($[\text{H}_2\text{SO}_4] =$
407 10^6 cm^{-3} and $[\text{MEA}] = 10 \text{ ppt}$) (right panel) as a function of relative humidity at 278.15
408 K.

409 **Atmospheric Implications.** We found that MEA at ppt-level can enhance the H₂SO₄-
410 based NPF. The enhancing potential of MEA for NPF is lower than that of DMA, which
411 is one of the strongest agents for enhancing H₂SO₄-based NPF,^{25,43} and much higher
412 than that of MA. In addition, we have shown that the -OH group of MEA plays an
413 important role in enhancing H₂SO₄-based NPF due to the formation of additional H-
414 bonds with H₂SO₄. To the best of our knowledge, this is the first study to point out the
415 significant effect of one additional functional group in amines and show that the basicity
416 of bases is not necessarily the only determining factor influencing H₂SO₄ driven NPF.
417 Besides anthropogenic emission,⁶⁷ the oxidation of aliphatic amines could introduce -
418 OH or keto-, peroxy- and carboxylic acid groups in the atmosphere.^{31,68,69} Amines
419 including these additional H-bond donor/acceptor functional groups can enhance the

420 NPF via a synergetic role of the basicity and the formation of additional H-bonds,
421 especially for strongly basic amines. As the enhancing effect is very dependent on the
422 exact structure of the molecule, the effect of these amines on NPF deserves further
423 investigation.

424 Obviously, the participation of MEA in H₂SO₄-based NPF is a sink of the emitted
425 MEA. It is known that the reaction with ·OH is an important sink for MEA due to a
426 high reaction rate constant ($k_{OH} 8.1 \times 10^{-11} \text{ cm}^3\text{molecule}^{-1}\text{s}^{-1}$ at 278.15 K) and
427 concentration of ·OH ($9.7 \times 10^5 \text{ cm}^{-3}$).¹⁸ At daytime, H₂SO₄ and ·OH can coexist in the
428 atmosphere and atmospheric concentration of H₂SO₄ (1×10^6 - $1.9 \times 10^7 \text{ cm}^{-3}$ depending
429 on the location)⁷⁰⁻⁷² is usually 1-19 times that of ·OH. We estimated the relative
430 contribution of H₂SO₄ to ·OH for the removal of MEA by $k_{H_2SO_4}[H_2SO_4]/k_{OH}[\cdot OH]$ at
431 278.15 K, where $k_{H_2SO_4}$ is removal rate constants of MEA for the participation in NPF
432 involving H₂SO₄ and its value is estimated to be 2.16×10^{-11} and $5.6 \times 10^{-11} \text{ cm}^3 \text{ molecule}^{-1}$
433 s^{-1} at dry or 50% RH condition, respectively (computational details in SI), [H₂SO₄]
434 and [·OH] are the concentration of H₂SO₄ and ·OH, respectively. The contribution of
435 H₂SO₄ to the removal of MEA is calculated to be about 0.27-5.2 and 0.7-13.1 times that
436 of ·OH at dry and 50% RH condition, respectively. This means that reactions with
437 H₂SO₄ will compete with oxidation by ·OH in the atmosphere for the removal of MEA
438 at tropospheric condition. Especially in regions where the concentration of H₂SO₄ is
439 high, NPF might be the dominant removal process of gas-phase MEA. Therefore, the
440 participation of MEA in H₂SO₄-based NPF should be considered when assessing the

441 environmental risk of MEA emissions related to, for example, postcombustion CO₂
442 capture technology.

443 **ASSOCIATED CONTENT**

444 **Supporting Information.** Details for boundary conditions, discussion on the stability
445 of cluster, hydration free energies, removal rate constants of MEA in NPF of H₂SO₄,
446 thermochemical information for the formation of molecular clusters, evaporation
447 coefficients for all evaporation pathways of different clusters, lower energy structures
448 for NH₃-H₂SO₄ and dimethylamine (DMA)-H₂SO₄, low energy structure involving the
449 hydrogen bonds between -OH of all MEA and H₂SO₄, Formation free energies for the
450 clusters for MA/NH₃-H₂SO₄, evaporation rates for MA/DMA-H₂SO₄ clusters, the
451 cluster formation rates and steady-state H₂SO₄ dimer concentrations as a function of
452 temperature, the main clustering pathways for MA/DMA-H₂SO₄ clusters, hydrate
453 distribution of clusters and coordinates of all optimized clusters. This material is
454 available free of charge via the Internet at <http://pubs.acs.org>.

455 **AUTHOR INFORMATION**

456 **Corresponding Author**

457 *Phone/fax: +86-411-84707844; e-mail: hbxie@dlut.edu.cn.

458 **ACKNOWLEDGEMENTS**

459 We thank the National Natural Science Foundation of China (21677028, 21325729)
460 and ERC 692891-DAMOCLES. We thank the CSC-IT Center for Science in Espoo,
461 Finland, for computational resources, Jonas Elm thanks the Carlsberg Foundation for
462 financial support and Hong-Bin Xie thanks the China Scholarship Council.

463 **REFERENCES**

- 464 (1) Veawab, A.; Tontiwachwuthikul, P.; Chakma, A., Corrosion Behavior of Carbon
465 Steel in the CO₂ Absorption Process Using Aqueous Amine Solutions. *Ind. Eng. Chem.*
466 *Res.* **1999**, *38* (10), 3917-3924.
- 467 (2) Liu, Y.; Zhang, L.; Watanasiri, S., Representing Vapor–Liquid Equilibrium for an
468 Aqueous MEA-CO₂ System Using the Electrolyte Nonrandom-Two-Liquid Model.
469 *Ind. Eng. Chem. Res.* **1999**, *38* (5), 2080-2090.
- 470 (3) Puxty, G.; Rowland, R.; Allport, A.; Yang, Q.; Bown, M.; Burns, R.; Maeder, M.;
471 Attalla, M., Carbon Dioxide Postcombustion Capture: A Novel Screening Study of
472 the Carbon Dioxide Absorption Performance of 76 Amines. *Environ. Sci. Technol.*
473 **2009**, *43* (16), 6427-6433.
- 474 (4) Xie, H.-B.; He, N.; Song, Z.; Chen, J.; Li, X., Theoretical Investigation on the
475 Different Reaction Mechanisms of Aqueous 2-Amino-2-methyl-1-propanol and
476 Monoethanolamine with CO₂. *Ind. Eng. Chem. Res.* **2014**, *53*, (8), 3363-3372.
- 477 (5) Xie, H.-B.; Johnson, J. K.; Perry, R. J.; Genovese, S.; Wood, B. R., A Computational
478 Study of the Heats of Reaction of Substituted Monoethanolamine with CO₂. *J. Phys.*
479 *Chem. A* **2011**, *115* (3), 342-350.
- 480 (6) Xie, H.-B.; Li, C.; He, N.; Wang, C.; Zhang, S.; Chen, J., Atmospheric Chemical
481 Reactions of Monoethanolamine Initiated by OH Radical: Mechanistic and Kinetic
482 Study. *Environ. Sci. Technol.* **2014**, *48* (3), 1700-1706.
- 483 (7) Xie, H.-B.; Wei, X.; Wang, P.; He, N.; Chen, J., CO₂ Absorption in an Alcoholic
484 Solution of Heavily Hindered Alkanolamine: The Reaction Mechanism of 2-(tert-
485 butylamino)- ethanol with CO₂ Revisited. *J. Phys. Chem. A* **2015**, *119*, 6346-6353
- 486 (8) Xie, H.-B.; Zhou, Y.; Zhang, Y.; Johnson, J. K., Reaction Mechanism of
487 Monoethanolamine with CO₂ in Aqueous Solution from Molecular Modeling. *J. Phys.*
488 *Chem. A* **2010**, *114*, (43), 11844-11852.
- 489 (9) da Silva, E. F.; Booth, A. M., Emissions from Postcombustion CO₂ Capture Plants.
490 *Environ. Sci. Technol.* **2013**, *47* (2), 659-660.
- 491 (10) Kapteina, S.; Slowik, K.; Verevkin, S. P.; Heintz, A., Vapor Pressures and
492 Vaporization Enthalpies of a Series of Ethanolamines. *J. Chem. Eng. Data* **2005**, *50* (2),
493 398-402.
- 494 (11) Karl, M.; Wright, R. F.; Berglen, T. F.; Denby, B., Worst Case Scenario Study to
495 Assess the Environmental Impact of Amine Emissions from a CO₂ Capture Plant. *Int.*
496 *J. Greenhouse Gas Control* **2011**, *5* (3), 439-447.
- 497 (12) Veltman, K.; Singh, B.; Hertwich, E. G., Human and Environmental Impact
498 Assessment of Postcombustion CO₂ Capture Focusing on Emissions from Amine-
499 Based Scrubbing Solvents to Air. *Environ. Sci. Technol.* **2010**, *44* (4), 1496-1502.
- 500 (13) Xie, H.-B.; Ma, F.; Wang, Y.; He, N.; Yu, Q.; Chen, J., Quantum Chemical Study
501 on ·Cl-Initiated Atmospheric Degradation of Monoethanolamine. *Environ. Sci.*
502 *Technol.* **2015**, *49* (22), 13246-13255.
- 503 (14) Karl, M.; Dye, C.; Schmidbauer, N.; Wisthaler, A.; Mikoviny, T.; D'Anna, B.;
504 Müller, M.; Borrás, E.; Clemente, E.; Muñoz, A.; Porras, R.; Ródenas, M.; Vázquez,

505 M.; Brauers, T., Study of OH-initiated Degradation of 2-aminoethanol. *Atmos. Chem.*
506 *Phys.* **2012**, *12* (4), 1881-1901.

507 (15) Karl, M.; Svendby, T.; Walker, S. E.; Velken, A. S.; Castell, N.; Solberg, S.,
508 Modelling atmospheric oxidation of 2-aminoethanol (MEA) emitted from post-
509 combustion capture using WRF–Chem. *Sci. Total Environ.* **2015**, 527–528, 185-202.

510 (16) Nielsen, C. J.; D’Anna, B.; Dye, C.; Graus, M.; Karl, M.; King, S.; Maguto, M.
511 M.; Müller, M.; Schmidbauer, N.; Stenström, Y.; Wisthaler, A.; Pedersen, S.,
512 Atmospheric chemistry of 2-aminoethanol (MEA). *Energy Proc.* **2011**, *4*, 2245-2252.

513 (17) Nielsen, C. J.; Herrmann, H.; Weller, C., Atmospheric Chemistry and
514 Environmental Impact of the Use of Amines in Carbon Capture and Storage (CCS).
515 *Chem. Soc. Rev.* **2012**, *41* (19), 6684-6704.

516 (18) Onel, L.; Blitz, M. A.; Seakins, P. W., Direct Determination of the Rate Coefficient
517 for the Reaction of OH Radicals with Monoethanol Amine (MEA) from 296 to 510 K.
518 *J. Phys. Chem. Lett.* **2012**, *3* (7), 853-856.

519 (19) Borduas, N.; Abbatt, J. P. D.; Murphy, J. G., Gas Phase Oxidation of
520 Monoethanolamine (MEA) with OH Radical and Ozone: Kinetics, Products, and
521 Particles. *Environ. Sci. Technol.* **2013**, *47* (12), 6377-6383.

522 (20) da Silva, G., Atmospheric Chemistry of 2-Aminoethanol (MEA): Reaction of the
523 $\text{NH}_2\text{CHCH}_2\text{OH}$ Radical with O_2 . *J. Phys. Chem. A* **2012**, *116* (45), 10980-10986.

524 (21) Manzoor, S.; Simperler, A.; Korre, A., A Theoretical Study of the Reaction
525 Kinetics of Amines Released into the Atmosphere from CO_2 Capture. *Int. J.*
526 *Greenhouse Gas Control* **2015**, *41*, 219-228.

527 (22) Onel, L.; Blitz, M. A.; Breen, J.; Rickard, A. R.; Seakins, P. W., Branching Ratios
528 for the Reactions of OH with Ethanol Amines Used in Carbon Capture and the Potential
529 Impact on Carcinogen Formation in the Emission Plume from a Carbon Capture Plant.
530 *Phys. Chem. Chem. Phys.* **2015**, *17* (38), 25342-25353.

531 (23) Zhang, R.; Suh, I.; Zhao, J.; Zhang, D.; Fortner, E. C.; Tie, X.; Molina, L. T.;
532 Molina, M. J., Atmospheric New Particle Formation Enhanced by Organic Acids.
533 *Science* **2004**, *304* (5676), 1487-1490.

534 (24) Winkler, P. M.; Steiner, G.; Vrtala, A.; Vehkamäki, H.; Noppel, M.; Lehtinen, K.
535 E. J.; Reischl, G. P.; Wagner, P. E.; Kulmala, M., Heterogeneous Nucleation
536 Experiments Bridging the Scale from Molecular Ion Clusters to Nanoparticles. *Science*
537 **2008**, *319*, (5868), 1374-1377.

538 (25) Almeida, J.; Schobesberger, S.; Kurten, A.; Ortega, I. K.; Kupiainen-Maatta, O.;
539 Praplan, A. P.; Adamov, A.; Amorim, A.; Bianchi, F.; Breitenlechner, M.; David, A.;
540 Dommen, J.; Donahue, N. M.; Downard, A.; Dunne, E.; Duplissy, J.; Ehrhart, S.;
541 Flagan, R. C.; Franchin, A.; Guida, R.; Hakala, J.; Hansel, A.; Heinritzi, M.; Henschel,
542 H.; Jokinen, T.; Junninen, H.; Kajos, M.; Kangasluoma, J.; Keskinen, H.; Kupc, A.;
543 Kurten, T.; Kvashin, A. N.; Laaksonen, A.; Lehtipalo, K.; Leiminger, M.; Leppa, J.;
544 Loukonen, V.; Makhmutov, V.; Mathot, S.; McGrath, M. J.; Nieminen, T.; Olenius, T.;
545 Onnela, A.; Petaja, T.; Riccobono, F.; Riipinen, I.; Rissanen, M.; Rondo, L.;
546 Ruuskanen, T.; Santos, F. D.; Sarnela, N.; Schallhart, S.; Schnitzhofer, R.; Seinfeld, J.

547 H.; Simon, M.; Sipila, M.; Stozhkov, Y.; Stratmann, F.; Tome, A.; Trostl, J.;
548 Tsagkogeorgas, G.; Vaattovaara, P.; Viisanen, Y.; Virtanen, A.; Vrtala, A.; Wagner, P.
549 E.; Weingartner, E.; Wex, H.; Williamson, C.; Wimmer, D.; Ye, P.; Yli-Juuti, T.;
550 Carslaw, K. S.; Kulmala, M.; Curtius, J.; Baltensperger, U.; Worsnop, D. R.;
551 Vehkamäki, H.; Kirkby, J., Molecular Understanding of Sulphuric Acid-amine Particle
552 Nucleation in the Atmosphere. *Nature* **2013**, *502* (7471), 359-363.

553 (26) Ehn, M.; Thornton, J. A.; Kleist, E.; Sipila, M.; Junninen, H.; Pullinen, I.; Springer,
554 M.; Rubach, F.; Tillmann, R.; Lee, B.; Lopez-Hilfiker, F.; Andres, S.; Acir, I.-H.;
555 Rissanen, M.; Jokinen, T.; Schobesberger, S.; Kangasluoma, J.; Kontkanen, J.;
556 Nieminen, T.; Kurten, T.; Nielsen, L. B.; Jorgensen, S.; Kjaergaard, H. G.; Canagaratna,
557 M.; Maso, M. D.; Berndt, T.; Petaja, T.; Wahner, A.; Kerminen, V.-M.; Kulmala, M.;
558 Worsnop, D. R.; Wildt, J.; Mentel, T. F., A Large Source of Low-volatility Secondary
559 Organic Aerosol. *Nature* **2014**, *506*, (7489), 476-479.

560 (27) Wang, Y. H.; Liu, Z. R.; Zhang, J. K.; Hu, B.; Ji, D. S.; Yu, Y. C.; Wang, Y. S.,
561 Aerosol Physicochemical Properties and Implications for Visibility During an Intense
562 Haze Episode During Winter in Beijing. *Atmos. Chem. Phys.* **2015**, *15*, (6), 3205-3215.

563 (28) Kirkby, J.; Curtius, J.; Almeida, J.; Dunne, E.; Duplissy, J.; Ehrhart, S.; Franchin,
564 A.; Gagne, S.; Ickes, L.; Kurten, A.; Kupc, A.; Metzger, A.; Riccobono, F.; Rondo, L.;
565 Schobesberger, S.; Tsagkogeorgas, G.; Wimmer, D.; Amorim, A.; Bianchi, F.;
566 Breitenlechner, M.; David, A.; Dommen, J.; Downard, A.; Ehn, M.; Flagan, R. C.;
567 Haider, S.; Hansel, A.; Hauser, D.; Jud, W.; Junninen, H.; Kreissl, F.; Kvashin, A.;
568 Laaksonen, A.; Lehtipalo, K.; Lima, J.; Lovejoy, E. R.; Makhmutov, V.; Mathot, S.;
569 Mikkilä, J.; Minginette, P.; Mogo, S.; Nieminen, T.; Onnela, A.; Pereira, P.; Petaja, T.;
570 Schnitzhofer, R.; Seinfeld, J. H.; Sipila, M.; Stozhkov, Y.; Stratmann, F.; Tome, A.;
571 Vanhanen, J.; Viisanen, Y.; Vrtala, A.; Wagner, P. E.; Walther, H.; Weingartner, E.;
572 Wex, H.; Winkler, P. M.; Carslaw, K. S.; Worsnop, D. R.; Baltensperger, U.; Kulmala,
573 M., Role of Sulphuric Acid, Ammonia and Galactic Cosmic Rays in Atmospheric
574 Aerosol Nucleation. *Nature* **2011**, *476* (7361), 429-433.

575 (29) Kurtén, T.; Loukonen, V.; Vehkamäki, H.; Kulmala, M., Amines Are Likely to
576 Enhance Neutral and Ion-induced Sulfuric Acid-water Nucleation in the Atmosphere
577 more Effectively than Ammonia. *Atmos. Chem. Phys.* **2008**, *8* (14), 4095-4103.

578 (30) Loukonen, V.; Kurtén, T.; Ortega, I. K.; Vehkamäki, H.; Pádua, A. A. H.; Sellegri,
579 K.; Kulmala, M., Enhancing Effect of Dimethylamine in Sulfuric Acid Nucleation in
580 the Presence of Water – a Computational Study. *Atmos. Chem. Phys.* **2010**, *10* (10),
581 4961-4974.

582 (31) Murphy, S. M.; Sorooshian, A.; Kroll, J. H.; Ng, N. L.; Chhabra, P.; Tong, C.;
583 Surratt, J. D.; Knipping, E.; Flagan, R. C.; Seinfeld, J. H., Secondary Aerosol Formation
584 from Atmospheric Reactions of Aliphatic Amines. *Atmos. Chem. Phys.* **2007**, *7* (9),
585 2313-2337.

586 (32) Berndt, T.; Stratmann, F.; Sipilä, M.; Vanhanen, J.; Petäjä, T.; Mikkilä, J.; Grüner,
587 A.; Spindler, G.; Lee Mauldin Iii, R.; Curtius, J.; Kulmala, M.; Heintzenberg, J.,
588 Laboratory Study on New Particle Formation from the Reaction OH + SO₂: Influence

589 of Experimental Conditions, H₂O Vapour, NH₃ and the Amine Tert-butylamine on the
590 Overall Process. *Atmos. Chem. Phys.* **2010**, *10* (15), 7101-7116.

591 (33) Smith, J. N.; Barsanti, K. C.; Friedli, H. R.; Ehn, M.; Kulmala, M.; Collins, D. R.;
592 Scheckman, J. H.; Williams, B. J.; McMurry, P. H., Observations of Aminium Salts in
593 Atmospheric Nanoparticles and Possible Climatic Implications. *Proc. Natl. Acad. Sci.*
594 **2010**, *107* (15), 6634-6639.

595 (34) Zhao, J.; Smith, J. N.; Eisele, F. L.; Chen, M.; Kuang, C.; McMurry, P. H.,
596 Observation of Neutral Sulfuric Acid-amine Containing Clusters in Laboratory and
597 Ambient Measurements. *Atmos. Chem. Phys.* **2011**, *11* (21), 10823-10836.

598 (35) Erupe, M. E.; Viggiano, A. A.; Lee, S. H., The Effect of Trimethylamine on
599 Atmospheric Nucleation Involving H₂SO₄. *Atmos. Chem. Phys.* **2011**, *11* (10), 4767-
600 4775.

601 (36) Lehtipalo, K.; Rondo, L.; Kontkanen, J.; Schobesberger, S.; Jokinen, T.; Sarnela,
602 N.; Kürten, A.; Ehrhart, S.; Franchin, A.; Nieminen, T.; Riccobono, F.; Sipilä, M.; Yli-
603 Juuti, T.; Duplissy, J.; Adamov, A.; Ahlm, L.; Almeida, J.; Amorim, A.; Bianchi, F.;
604 Breitenlechner, M.; Dommen, J.; Downard, A. J.; Dunne, E. M.; Flagan, R. C.; Guida,
605 R.; Hakala, J.; Hansel, A.; Jud, W.; Kangasluoma, J.; Kerminen, V.-M.; Keskinen, H.;
606 Kim, J.; Kirkby, J.; Kupc, A.; Kupiainen-Määttä, O.; Laaksonen, A.; Lawler, M. J.;
607 Leiminger, M.; Mathot, S.; Olenius, T.; Ortega, I. K.; Onnela, A.; Petäjä, T.; Praplan,
608 A.; Rissanen, M. P.; Ruuskanen, T.; Santos, F. D.; Schallhart, S.; Schnitzhofer, R.;
609 Simon, M.; Smith, J. N.; Tröstl, J.; Tsagkogeorgas, G.; Tomé, A.; Vaattovaara, P.;
610 Vehkamäki, H.; Vrtala, A. E.; Wagner, P. E.; Williamson, C.; Wimmer, D.; Winkler,
611 P. M.; Virtanen, A.; Donahue, N. M.; Carslaw, K. S.; Baltensperger, U.; Riipinen, I.;
612 Curtius, J.; Worsnop, D. R.; Kulmala, M., The Effect of Acid–base Clustering and Ions
613 on the Growth of Atmospheric Nano-particles. *Nat. Commun.* **2016**, *7*, 11594.

614 (37) Chen, M.; Titcombe, M.; Jiang, J.; Jen, C.; Kuang, C.; Fischer, M. L.; Eisele, F.
615 L.; Siepmann, J. I.; Hanson, D. R.; Zhao, J.; McMurry, P. H., Acid–base Chemical
616 Reaction Model for Nucleation Rates in the Polluted Atmospheric Boundary Layer.
617 *Proc. Natl. Acad. Sci.* **2012**, *109* (46), 18713-18718.

618 (38) Xu, Z.-Z.; Fan, H.-J., Competition Between H₂SO₄-(CH₃)₃N and H₂SO₄-H₂O
619 Interactions: Theoretical Studies on the Clusters [(CH₃)₃N]·(H₂SO₄)·(H₂O)₃₋₇. *J. Phy.*
620 *Chem. A* **2015**, *119* (34), 9160-9166.

621 (39) Lv, S.-S.; Miao, S.-K.; Ma, Y.; Zhang, M.-M.; Wen, Y.; Wang, C.-Y.; Zhu, Y.-P.;
622 Huang, W., Properties and Atmospheric Implication of Methylamine–Sulfuric Acid–
623 Water Clusters. *J. Phy. Chem. A* **2015**, *119* (32), 8657-8666.

624 (40) Nadykto, A.; Yu, F.; Jakovleva, M.; Herb, J.; Xu, Y., Amines in the Earth’s
625 Atmosphere: A Density Functional Theory Study of the Thermochemistry of Pre-
626 Nucleation Clusters. *Entropy* **2011**, *13* (2), 554-569.

627 (41) Nadykto, A.; Herb, J.; Yu, F.; Xu, Y.; Nazarenko, E., Estimating the Lower Limit
628 of the Impact of Amines on Nucleation in the Earth’s Atmosphere. *Entropy* **2015**, *17*(5),
629 2764-2780.

630 (42) Nadykto, A. B.; Herb, J.; Yu, F.; Xu, Y., Enhancement in the Production of
631 Nucleating Clusters due to Dimethylamine and Large Uncertainties in the
632 Thermochemistry of Amine-enhanced Nucleation. *Chem. Phys. Lett.* **2014**, *609*, 42-49.
633 (43) Jen, C. N.; McMurry, P. H.; Hanson, D. R., Stabilization of Sulfuric Acid Dimers
634 by Ammonia, Methylamine, Dimethylamine, and Trimethylamine. *J. Geophys. Res.*
635 *Atmos.* **2014**, *119* (12), 7502-7514.
636 (44) Jen, C. N.; Bachman, R.; Zhao, J.; McMurry, P. H.; Hanson, D. R., Diamine-
637 sulfuric Acid Reactions Are a Potent Source of New Particle Formation. *Geophys. Res.*
638 *Lett.* **2016**, *43* (2), 867-873.
639 (45) Elm, J.; Jen, C. N.; Kurtén, T.; Vehkamäki, H., Strong Hydrogen Bonded
640 Molecular Interactions between Atmospheric Diamines and Sulfuric Acid. *J. Phy.*
641 *Chem. A* **2016**, *120* (20), 3693-3700.
642 (46) Hall, H. K., Correlation of the Base Strengths of Amines I. *J. Am. Chem. Soc.* **1957**,
643 *79* (20), 5441-5444.
644 (47) McGrath, M. J.; Olenius, T.; Ortega, I. K.; Loukonen, V.; Paasonen, P.; Kurtén,
645 T.; Kulmala, M.; Vehkamäki, H., Atmospheric Cluster Dynamics Code: a flexible
646 method for solution of the birth-death equations. *Atmos. Chem. Phys.* **2012**, *12* (5),
647 2345-2355.
648 (48) Olenius T, K.-M. O. I., Kurtén T, Vehkamäki H., Free Energy Barrier in the
649 Growth of Sulfuric Acid–ammonia and Sulfuric Acid–dimethylamine Clusters. *J.*
650 *Chem. Phys.* **2013**, *139* (8), 084312.
651 (49) Ortega, I. K.; Kupiainen, O.; Kurtén, T.; Olenius, T.; Wilkman, O.; McGrath, M.
652 J.; Loukonen, V.; Vehkamäki, H., From Quantum Chemical Formation Free Energies
653 to Evaporation Rates. *Atmos. Chem. Phys.* **2012**, *12* (1), 225-235.
654 (50) Elm, J.; Fard, M.; Bilde, M.; Mikkelsen, K. V., Interaction of Glycine with
655 Common Atmospheric Nucleation Precursors. *J. Phy. Chem. A* **2013**, *117* (48), 12990-
656 12997.
657 (51) Elm, J.; Mylly, N.; Hyttinen, N.; Kurtén, T., Computational Study of the
658 Clustering of a Cyclohexene Autoxidation Product C₆H₈O₇ with Itself and Sulfuric
659 Acid. *J. Phy. Chem. A* **2015**, *119* (30), 8414-8421.
660 (52) Frisch, M. J.; Trucks, G. W.; H.B, S.; Scuseria, G. E.; Robb, M. A.; Cheeseman,
661 J. R., et.al *Gaussian 09*, 2009
662 (53) Elm, J.; Bilde, M.; Mikkelsen, K. V., Assessment of Binding Energies of
663 Atmospherically Relevant Clusters. *Phys. Chem. Chem. Phys.* **2013**, *15* (39), 16442-
664 16445.
665 (54) Elm, J.; Kristensen, K., Basis Set Convergence of the Binding Eenergies of
666 Strongly Hydrogen-bonded Atmospheric Clusters. *Phys. Chem. Chem. Phys.* **2017**, *19*
667 (2), 1122-1133.
668 (55) Riplinger, C.; Neese, F., An Efficient and Near Linear Scaling Pair Natural Orbital
669 Based Local Coupled Cluster Method. *J. Chem. Phys.* **2013**, *138* (3), 034106.

670 (56) Riplinger, C.; Sandhoefer, B.; Hansen, A.; Neese, F., Natural Triple Excitations in
671 Local Coupled Cluster Calculations with Pair Natural Orbitals. *J. Chem. Phys.* **2013**,
672 *139* (13), 134101.

673 (57) Neese, F., The ORCA program system. *Wiley Interdiscip. Rev. Comput. Mol. Sci.*
674 **2012**, *2* (1), 73-78.

675 (58) Mylly, N.; Elm, J.; Halonen, R.; Kurtén, T.; Vehkamäki, H., Coupled Cluster
676 Evaluation of the Stability of Atmospheric Acid–Base Clusters with up to 10
677 Molecules. *J. Phy. Chem. A* **2016**, *120* (4), 621-630.

678 (59) Vorobyov, I.; Yappert, M. C.; DuPré, D. B., Hydrogen Bonding in Monomers and
679 Dimers of 2-Aminoethanol. *J. Phy. Chem. A* **2002**, *106* (4), 668-679.

680 (60) Tinja Olenius, Roope Halonen, Theo Kurtén, Henning Henschel, Oona Kupiainen-
681 Määttä, Ismael K. Ortega, Hanna Vehkamäki, and Ilona Riipinen, New Particle
682 Formation from Sulfuric Acid and Amines: Comparison of Mono-, Di-, and
683 Trimethylamines. *Submitted to Journal of Geophysical Research: Atmospheres*.

684 (61) Henschel, H.; Kurtén, T.; Vehkamäki, H., Computational Study on the Effect of
685 Hydration on New Particle Formation in the Sulfuric Acid/Ammonia and Sulfuric
686 Acid/Dimethylamine Systems. *J. Phy. Chem. A* **2016**, *120* (11), 1886-1896.

687 (62) Kerminen, V. M.; Petäjä, T.; Manninen, H. E.; Paasonen, P.; Nieminen, T.; Sipilä,
688 M.; Junninen, H.; Ehn, M.; Gagné, S.; Laakso, L.; Riipinen, I.; Vehkamäki, H.; Kurten,
689 T.; Ortega, I. K.; Dal Maso, M.; Brus, D.; Hyvärinen, A.; Lihavainen, H.; Leppä, J.;
690 Lehtinen, K. E. J.; Mirme, A.; Mirme, S.; Hörrak, U.; Berndt, T.; Stratmann, F.; Birmili,
691 W.; Wiedensohler, A.; Metzger, A.; Dommen, J.; Baltensperger, U.; Kiendler-Scharr,
692 A.; Mentel, T. F.; Wildt, J.; Winkler, P. M.; Wagner, P. E.; Petzold, A.; Minikin, A.;
693 Plass-Dülmer, C.; Pöschl, U.; Laaksonen, A.; Kulmala, M., Atmospheric Nucleation:
694 Highlights of the EUCAARI Project and Future Directions. *Atmos. Chem. Phys.* **2010**,
695 *10* (22), 10829-10848.

696 Chen, H.; Varner, M. E.; Gerber, R. B.; Finlayson-Pitts, B. J., Reactions of
697 Methanesulfonic Acid with Amines and Ammonia as a Source of New Particles in Air.
698 *J. Phys. Chem. B* **2016**, *120*(8), 1526-1536.

699 (64) Ling, J.; Ding, X.; Li, Z.; Yang, J., First-Principles Study of Molecular Clusters
700 Formed by Nitric Acid and Ammonia. *J. Phy. Chem. A* **2017**, *121* (3), 661-668.

701 (65) DePalma, J. W.; Wang, J.; Wexler, A. S.; Johnston, M. V., Growth of Ammonium
702 Bisulfate Clusters by Adsorption of Oxygenated Organic Molecules. *J. Phy. Chem. A*
703 **2015**, *119* (45), 11191-11198.

704 (66) DePalma, J. W.; Doren, D. J.; Johnston, M. V., Formation and Growth of
705 Molecular Clusters Containing Sulfuric Acid, Water, Ammonia, and Dimethylamine.
706 *J. Phy. Chem. A* **2014**, *118* (29), 5464-5473.

707 (67) Ge, X.; Wexler, A. S.; Clegg, S. L., Atmospheric Amines – Part I. A review. *Atmos.*
708 *Environ.* **2011**, *45* (3), 524-546.

709 (68) Price, D. J.; Clark, C. H.; Tang, X.; Cocker, D. R.; Purvis-Roberts, K. L.; Silva, P.
710 J., Proposed Chemical Mechanisms leading to Secondary Organic Aerosol in the

711 Reactions of Aliphatic Amines with Hydroxyl and Nitrate Radicals. *Atmos. Environ.*
712 **2014**, 96, 135-144.

713 (69) Angelino, S.; Suess, D. T.; Prather, K. A., Formation of Aerosol Particles from
714 Reactions of Secondary and Tertiary Alkylamines: Characterization by Aerosol Time-
715 of-Flight Mass Spectrometry. *Environ. Sci. Technol.* **2001**, 35 (15), 3130-3138.

716 (70) Zheng, J.; Hu, M.; Zhang, R.; Yue, D.; Wang, Z.; Guo, S.; Li, X.; Bohn, B.; Shao,
717 M.; He, L.; Huang, X.; Wiedensohler, A.; Zhu, T., Measurements of Gaseous H₂SO₄
718 by AP-ID-CIMS During CAREBeijing 2008 Campaign. *Atmos. Chem. Phys.* **2011**, 11
719 (15), 7755-7765.

720 (71) Berresheim, H.; Elste, T.; Tremmel, H. G.; Allen, A. G.; Hansson, H. C.; Rosman,
721 K.; Dal Maso, M.; Mäkelä, J. M.; Kulmala, M.; O'Dowd, C. D., Gas-aerosol
722 relationships of H₂SO₄, MSA, and OH: Observations in the Coastal Marine Boundary
723 Layer at Mace Head, Ireland. *J. Geophys. Res. Atmos.* **2002**, 107 (D19), PAR 5-1-PAR
724 5-12.

725 (72) Jokinen, T.; Sipilä, M.; Junninen, H.; Ehn, M.; Lönn, G.; Hakala, J.; Petäjä, T.;
726 Mauldin Iii, R. L.; Kulmala, M.; Worsnop, D. R., Atmospheric Sulphuric Acid and
727 Neutral Cluster Measurements Using CI-API-TOF. *Atmos. Chem. Phys.* **2012**, 12, (9),
728 4117-4125.